INTERNATIONAL JOURNAL OF PRECISION ENGINEERING AND MANUFACTURING Vol. 16, No. 10, pp. 2179-2184 SEPTEMBER 2015 / 2179
DOI: 10.1007/s12541-015-0280-1 ISSN 2234-7593 (Print) / ISSN 2005-4602 (Online)

A Study on the Fracture Characteristics of Tapered Double Cantilever Specimens Bonded with Aluminum Foams of Varying Thicknesses

Hong Peng Sun[1] and Jae Ung Cho[2,#]

1 Department of Mechanical Engineering, Graduate School, Kongju National University, 1223-24, Cheonan-daero, Seobuk-gu, Cheonan-si, Chungcheongnam-do, 331-717, South Korea
2 Division of Mechanical & Automotive Engineering, Kongju National University, 1223-24, Cheonan-daero, Seobuk-gu, Cheonan-si, Chungcheongnam-do, 331-717, South Korea
Corresponding Author / E-mail: jucho@kongju.ac.kr, TEL: +82-41-521-9271, FAX: +82-41-555-9123

KEYWORDS: Aluminum foam, TDCB (Tapered double cantilever beam) specimen, Fracture characteristic, Reaction force, Bonded interface, Porous core

In this study, the fracture characteristics on the adhesive interfaces in the structures composed of aluminum foam were investigated by using three kinds of TDCB specimens with the thicknesses of 25 mm, 50 mm and 75 mm and the length of 200 mm. According to the test results for the 25 mm-thick specimens, the maximum reaction force of about 200 N was shown when forced displacement progressed as the amount of about 6 mm to 7 mm. And the reaction force nearly was disappeared after the forced displacement progressed as the amount of about 22 mm. Similar trends were observed in cases of other specimens with thicknesses of 50 mm and 75 mm. As the forced displacement was gradually increased,fractures began to occur with the separation from the bonded interface beginning when the equivalent stress happened at the bonded interface was larger than the adhesive stress of 0.167 MPa at the bonding interface. Such experimental results can be verified by simulation analysis results. Therefore, fracture characteristics of aluminum foam consisting of the porous cores are considered to be identifiable through only simulations instead of experiments without requiring significant cost or time.

Manuscript received: March 14, 2015 / Revised: July 13, 2015 / Accepted: July 14, 2015

1. Introduction

Nowadays, many industries such as vehicles, transport, ship building have been developed. In these industries, mechanical apparatuses are also being developed. Unlike in the past when machines were designed from simple steels, the machine performance is being improved by using special alloy steels and composite materials. As designing machines requires identification of material characteristics to be used at the right time and in the right place, it has become a crucial task for machine designers. Transport machines are currently trending towards ultra-light weight and high performance. Therefore, it is necessary to develop new materials with excellent mechanical and thermal characteristics which can efficiently absorb impact energy that increases daily. As porous metal that comes from aluminum foam is the metallic material that has many cell lattices inside, it becomes an ultra-light metal because it is produced from foaming into a sponge shape with the addition of a thickener and a foaming agent. This product is produced after dissolving an aluminum ingot into the solution.[1-3] To obtain the lightest weight and optimal absorption function for impact energy, aluminum foam is widely used in a variety of areas. These areas include lightweight structures and other biomaterials, among other things, and they have many advantages such as low density, inflammability, high specific stiffness, an excellent energy absorption rate, acoustic absorption and low thermal conductivity. While pores found in metallic materials are generally considered a defect, they can be advantageous as lightweight materials if the pores are organized into uniform sizes and distributed by using foaming techniques. Recently, foam composite materials that have bubbles inside from adding a foaming agent to molten aluminum are rapidly used as a next-generation material. The materials are divided into two types depending on the formation of the cells. These two types are open-cell, which is used in heat transfer areas and the closed-cell type, which is commonly used as a shock absorber.[4-6] Since aluminum foam is unlike other materials in that it has many pores on its surface area, it is considered to greatly differ at its fracture characteristics from that of other bonded interfaces for general materials. Therefore, it is important to study the fracture of adhesive structures composed of aluminum foam and the fracture resistance of the bonded interface. To evaluate the strength of bonded

Fig. 1 Actual example for application of adhesive structure

joints, a widely used evaluation method uses the application of fracture mechanics. In this study, tapered double cantilever beam (TDCB) specimens have been traditionally employed to better understand the fracture characteristics of the bonded interface. These subjects include the shearing composite materials and the ability to measure fracture resistance values in cases where cracks are found from shearing.[7-9] Since Fig. 1 shows that the angles and areas of the bonded parts of various structures actually widely varied in how they bonded with an adhesive, TDCB specimens were designed so that specimen thickness would be set as a variable in this study. For models, there were 3 types; (a), (b) and (c), where the specimen length was 200 mm while the 3 models varied in thicknesses of 25 mm, 50 mm and 75 mm.

Also, TDCB specimens of aluminum foam composites were designed by applying the British industrial standard (BS 7991) and the ISO international standard (ISO 11343), and then Mode II tests were performed. 2D modeling of the same shape as the experimental specimens and the finite element analysis for comparison with the experimental results and for verification was performed. As a result, the shapes of breakage based on specimen fracture behavior that have TDCB shape bonded by adhesive are being investigated.

2. Model of Cohesive Zone Material

As for the model in this study, the bilinear law for tangential traction and separation in cohesive zone materials are applied. Fig. 2 shows that the relationship between load and displacement follows the OAC line. The triangular region under the OAC line indicates the critical fracture energy values.

The relation between tangential cohesive traction Tt and tangential displacement jump Ut can be expressed as Eq. (1).

$$T_t = K_t U_t (1 - d_t) \tag{1}$$

Where,

K_t = tangential cohesive stiffness $T_t^{max}/\overline{U_t}$

T_t^{max} = maximum tangential cohesive traction τ_{max}

$\overline{U_t}$ = tangential displacement jump at maximum tangential cohesive traction

U^c_t = tangential displacement jump at the completion of debonding

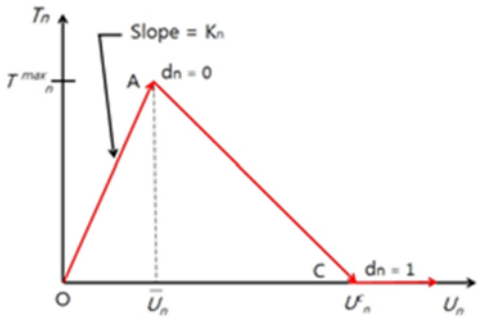

Fig. 2 Contact stress of material with bilinear cohesive zone

α = ratio of $\overline{U_t}$ to U^c_t

d_t = damage parameter associated with Mode II dominated bilinear cohesive law

3. Basic Theory on the Fracture Strength of Specimen

An equivalent stress for the specimens is shown by Von Mises stress on analysis. This stress is the value equivalent to the uniaxial stress based on three dimensional stress conditions. When this stress reaches its yield stress, breakage occurs. Whereas a principal stress has the magnitude and the direction as a vector, the equivalent stress is only measured by the magnitude. In the complex 3D model, yielding or rupture is only determined by an equivalent stress rather than a principal stress.[10,11] Strain energy theory states that the strain energy for the unit volume within a material becomes equal to the strain energy for the unit volume at the yield point when the breakage occurs in the case of simple tension. The condition for breakage according to the shear strain energy theory is as shown in Eq. (2). When the maximum equivalent stress is greater than the yield stress of the material, the breakage is expected to occur from at the beginning of the separation of bonding.[12-15]

$$\sigma_e^{\,2} = \frac{1}{2}\{(\sigma_1 - \sigma_2)^2 + (\sigma_2 - \sigma_3)^2 + (\sigma_3 - \sigma_1)^2\} \tag{2}$$

where, σ_e = Equivalent stress

σ_1 = Stress in axis 1 (x axis) direction

σ_2 = Stress in axis 2 (y axis) direction

σ_3 = Stress in axis 3 (z axis) direction

4. Experimental Methods

4.1 Experimental apparatus and experimental model

In this study, fracture experiments were conducted by using the Landmark tester of MTS company as shown by Fig. 3. Data from the experimental results were outputted by using a computer, and the pictures from the experiments for each specimen were filmed.

To reduce potential errors in experimental data, a few specimens were produced by individual case by Foam Tech Co., Ltd. of Korea So, the average values of experimental data were extracted with these specimens.[16,17] Fig. 4 shows the specimens that have the tapes attached

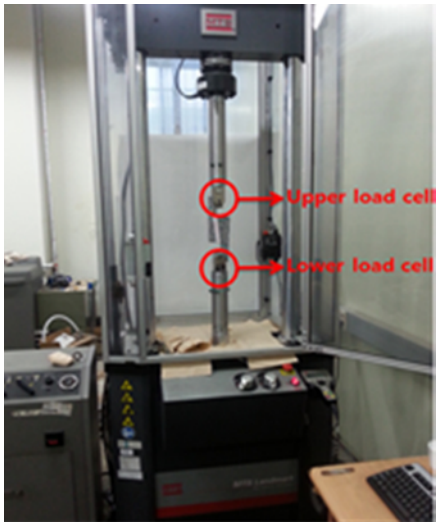

Fig. 3 Experimental setup

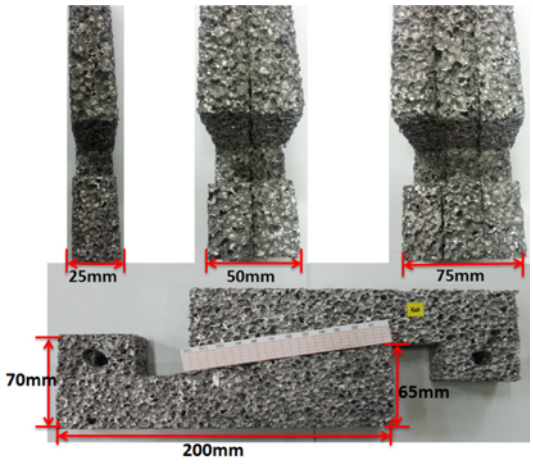

Fig. 4 Experimental specimens

Fig. 5 Experimental condition

Fig. 6 Test of adhesive strength at bonded interface

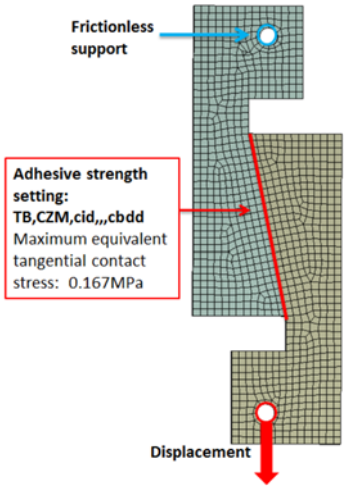

Fig. 7 FE model and constraint condition

to them for the purpose in order to measure the amount of cracks and their length. The experiment was carried out with these specimens at the state which was not out-of-plane but in-plane loading. In addition, the study was experimented with the specimens of varying Thicknesses. Therefore, these specimens can become the configuration of tapered double cantilevered beams modified from the basic cantilever beam.

As the experimental procedure, the specimen was mounted on a tension tester, as shown by Fig. 5. To induce shear cracking in a direction, a fixed load block was placed on one side for support, while another load block on the other side was set to be allowed to move down at the given displacement rate of 0.167 mm/s.

4.2 Numerical modeling

First, the initial experiments was performed as shown by Fig. 6 in order to input the adhesive stress of the maximum equivalent stress at the bonded interface between aluminum foams in ANSYS analysis program. According to the result of measurement, the bonded interface was separated due to rupture when the stress at the bonded interface with applied adhesive was greater than about 0.167 MPa. Thus, adhesion is considered to withstand stress up to this level and the adhesive stress for this bonded interface has been inputted into the program.

Table 1 Properties of aluminum foam

Property	Value
Density(kg/m^3)	400
Young's modulus(MPa)	2,374
Poisson's ratio	0.29
Yield strength(MPa)	1.8
Shear strength(MPa)	0.92

Table 2 Ingredients in the adhesive

Ingredients	Weight proportions (%)
Non-volatile component	20-30
Acetone	20-30
Propane	15-25
2-Methylpentane	10-20
Cyclohexane	3-7
3-Methylpentane	3-7
2,2-Dimethylbutane	1-3
2,3-Dimethylbutane	1-3
Hexane	<0.8

In this study, TDCB Mode II model was manufactured with the same specification as the actual specimens. The finite element model for this aluminum foam is the 2-dimensional model and it has been divided into square elements, as shown in Fig. 7. As shown by this figure, the model was secured at the pinhole on the upper load block while forced displacement was applied in the vertical direction to the pinhole of the lower load block. Also, material property values for the analytical model are shown in Table 1.[18] Table 2 shows the ingredients in the adhesive.

5. Analytical Results and Verification by Experiments for Consideration

5.1 Comparison between experiments and analytical results for 25 mm-thick aluminum foam

The experimental process and analytical process are as shown in Fig. 8. In these processes, the forced displacement progressed at a constant rate and these pictures were filmed by a camcorder while the experiment was being performed, according to experimental conditions. As the forced displacement was gradually increased, the bonded interface began to separate when the fracture occurred from the moment where the equivalent stress that was produced at the bonded interface became greater than the adhesive stress of 0.167 MPa at the bonded interface. By considering the experimental process of forced displacement, it can be seen that the tapered bonded interface of the specimen was completely fractured from the separation of two beams after the forced displacement exceeded more than approximately 22 mm. Also, according to the analytical process, the maximum equivalent stress was shown to become about 2.3 MPa when the forced displacement progressed by approximately 7 mm.

The experimental and analytical processes for specimens have been converted into data and are shown in Fig. 9. By considering this graph, the reaction force of the analytical data is shown to be nearly identical to the reaction force value of the experimental data. The maximum reaction force of the specimens when the forced displacement progressed by the amount of about 6 to 7 mm is shown to be about 200 N, and the

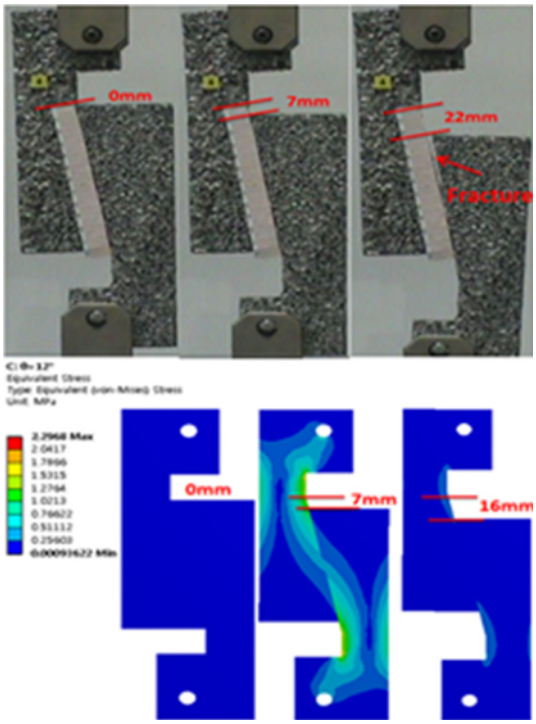

Fig. 8 Progression of displacement on specimen in experiment and simulation

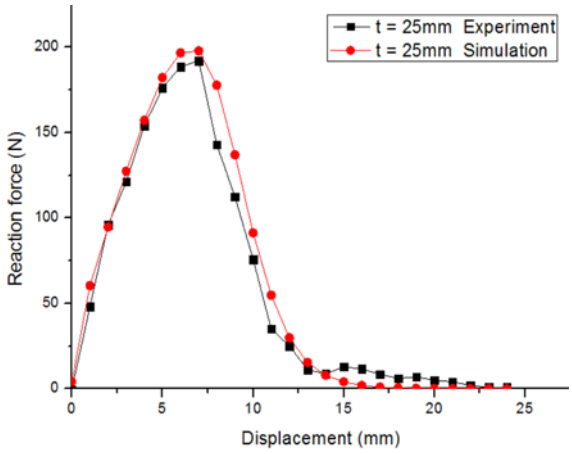

Fig. 9 Graph of displacement-force reaction (t=25 mm) in experiment and simulation

shear force is seen to be drastically reduced after the occurrence of the maximum reaction force. In this study, it is meaningfully thought that the maximum reactions of which the aluminum foam specimens can endure are examined. Also, it is helpful to design these kinds of real structures by referring these reaction forces. At the simulation graph of analysis data, the reaction force nearly disappeared after the progression of the forced displacement was about 16 mm, while the experimental data showed that the reaction force almost disappeared after progression of the forced displacement was about 22 mm. The reason for such a difference is attributable to the fact that adhesion inertia cannot be shown in the analysis while the adhesive remains without disappearing

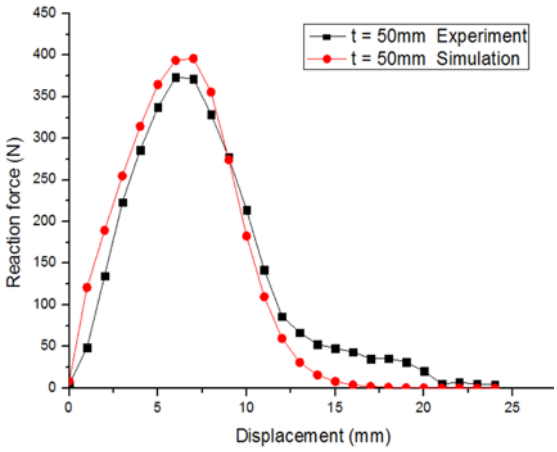

Fig. 10 Graph of displacement-force reaction (t=50 mm) in experiment and simulation

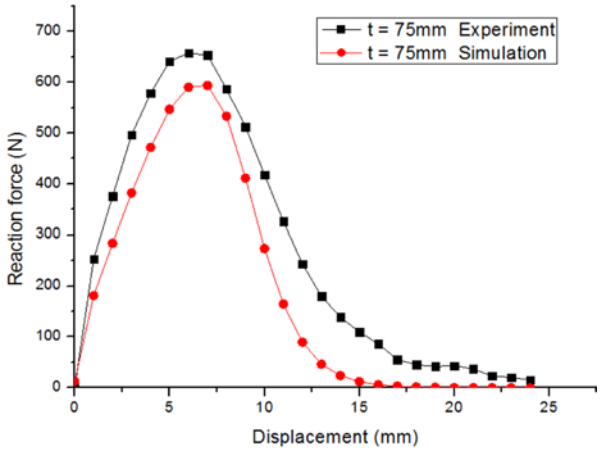

Fig. 11 Graph of displacement-force reaction (t=75 mm) in experiment and simulation

and so, some residual stress is still remained when the experiment is performed.

5.2 Comparison between experiments and analytical results for 50 mm-thick aluminum foam

Since the all three specimen types show similar aspects, only the experimental and the analytical processes for 25 mm-thick specimens are shown representatively as shown by Fig. 8. And the experimental and the analytical processes for 50 mm- and 75 mm-thick specimens are shown as the graphs following data formations. Fig. 10 shows the graph comparing experiment and analysis for 50 mm-thick specimens.

As shown by this figure, the maximum reaction forces of 370 N and 400 N at experiment and simulation is shown are shown respectively when the forced displacement proceeds as the amount as 6 to 7 mm. And the shear force is observed to be drastically reduced after the occurrence of the maximum reaction force. The maximum discrepancy of analysis data becomes about 8.1% in comparison with the experimental data. In the experiments, the reaction force nearly disappeared after the forced displacement progressed by about 21 mm, and the reaction force can be seen to almost disappear in the analysis when the forced displacement progressed by about 15 mm.

5.3 Comparison between experiments and analytical results for 75 mm-thick aluminum foam

Fig. 11 shows a graph comparing experiment and analysis for 75 mm-thick specimens. Although there is some differences between the experiments and the analytical results, similar results are produced as a whole. The reaction force could be seen to nearly disappear when the forced displacement progressed by about 23 mm after the maximum reaction force of about 660 N was observed when the forced displacement progressed by about 7 mm. As shown by this figure, the maximum reaction force of 595 N at simulation is shown and the maximum discrepancy of analysis data becomes about 9.1% in comparison with the experimental data. Although three types of TDCB specimens have different thicknesses in the X-axis direction, the displacement in the Z-axis direction is happened the load block, i.e., in the shear direction of the bonded interface. ‘X-axis’ is the direction of specimen thickness. And ‘Z-axis’ is the direction on which the loading block is applied, that is, the vertical direction. Therefore, the adhesive separation was happened in an identical way at the forced displacement of about 22 mm, irrespective of thicknesses for the three types of specimens.

When the tendency of the experimental and analytical results was applied to three models employed in this study, adhesive strengths of TDCB adhesive structures composed of aluminum foam in different thicknesses could be evaluated. It is considered that an analysis alone can be a method for allowing the prediction of structural safety for actual adhesive structures without the need to perform experiments.

6. Conclusion

In this study, the following conclusions can be drawn as a result of performing shear force experiments and analysis for TDCB specimens that were prepared with aluminum foam of varying thicknesses.

1. According to the experimental results for 25 mm-thick specimens, the specimens showed a maximum reaction force of about 200 N in the part where the forced displacement progressed by about 6~7 mm, and the reaction force nearly disappeared after the forced displacement progressed to about 22 mm.

2. According to the experimental results for specimen thicknesses of 50 mm and 75 mm, the maximum reaction forces after the progression of the forced displacement with the amount of about 6 mm to 7 mm were shown to be about 400 N and 650 N, respectively, and the reaction force nearly disappeared after the forced displacement progressed to about 22 mm.

3. According to comparison and verification by using the finite element analysis method, the resulting study values were shown to be nearly identical. Since the adhesive continued to remain without disappearing when the maximum reaction force was being reduced, some discrepancies occurred in the experimental graphs and analytical graphs. As the forced displacement was gradually increased, the bonded interface began to separate because of the occurrence of fractures from the moment where the equivalent stress produced at the bonded

interface became greater than the adhesive stress of 0.167 MPa. In addition, it was evident that identical separation occurred at the bonded interface, irrespective of the thicknesses of the three specimens when the forced displacement became approximately 22 mm.

4. Through this study, it can be affirmed that the resulting study values of the experiment and analysis do not differ each other. Therefore, instead of experiments that require a lot of cost and time, it is thought that the mechanical characteristics on specimen thicknesses of aluminum foam materials composed of the porous cores can be identified through the simulations by using such a method. Consequently, the result of this study for the breakage of functional composite material that have such diversified shapes are believed to be able to greatly contribute to the studies on composite materials, impact fractures.

ACKNOWLEDGEMENT

This research was supported by the Basic Science Research Program through the National Research Foundation of Korea (NRF) funded by the Ministry of Education, Science, and Technology (2011-0006548).

REFERENCES

1. Kim, D. Y., Kwak, J. H., Lee, J. H., Park, K. W., Jeong, K. Y., and Cheon, S. S., "A Study on the Vibration Analysis for the Composite Multi-Axial Optical Structure of an Aircraft," Composites Research, Vol. 24, No. 2, pp. 14-21, 2011.
2. British Standard Institution, "Determination of the Mode I Adhesive Fracture Energy Gic of Structure Adhesives using the Double Cantilever Beam (DCB) and Tapered Double Cantilever Beam (TDCB) Specimens," BS 7991, 2001.
3. Bang, S. O., Kim, K. S., Kim, S. H., Song, S. G., and Cho, J. U., "Study on Compression Tests of Aluminum Foam and Honeycomb Sandwich Composites," Journal of the Korea Academia-Industrial Cooperation Society, Vol. 12, No. 9, pp. 3802-3807, 2011.
4. Cho, H. Y., Kim, D. B., and Kim, K. W., "Shape Design of Self-Piercing Rivet for Joining Dissimilar Sheet Metals," Journal of Korea Society of Mechanical Technology, Vol. 14, No. 3, pp. 93-99, 2012.
5. Lee, J.-K., "Elastic Analysis in Composite including Multiple Elliptical Fibers," Composites Research, Vol. 24, No. 6, pp. 37-48, 2011.
6. Kim, J. G., Hwang, Y. J., and Yoon, S. H., "Improvement of the Fracture Toughness of Adhesively Bonded Stainless Steel Joints with Aramid Fibers at Cryogenic Temperatures," Composite Structures, Vol. 94, No. 9, pp. 2982-2989, 2012.
7. Kim, S. S., Han, M. S., Cho, J. U., and Cho, C. D., "Study on the Fatigue Experiment of TDCB Aluminum Foam Specimen Bonded with Adhesive," Int. J. Precis. Eng. Manuf., Vol. 14, No. 10, pp. 1791-1795, 2013.
8. Marzi, S., Biel, A., and Stigh, U., "On Experimental Methods to Investigate the Effect of Layer Thickness on the Fracture Behavior of Adhesively Bonded Joints," International Journal of Adhesion and Adhesives, Vol. 31, No. 8, pp. 840-850, 2011.
9. Hart-Smith, L., "Further Developments in the Design and Analysis of Adhesive-Bonded Structural Joints," Douglas Aircraft Co., McDonnell Douglas Corporation, Paper 6922, presented to ASTM Conference on Jointing of Composite Materials (STP 749), 1980.
10. Choi, H. K. and Cho, J. U., "Study on the Fatigue Analysis of DCB Model with Aluminum Foam," Journal of Korean Society of Mechanical Technology, Vol. 14, No. 6, pp. 39-43, 2012.
11. Zhang, Y. J. and Yang, C. S., "Fem Analyses for Influences of Stress-Chemical Solution on Thm Coupling in Dual-Porosity Rock Mass," Journal of Central South University, Vol. 19, No. 4, pp. 1138-1147, 2012.
12. Han, M. S., Choi, H. K., Cho, J. U., and Cho, C. D., "Experimental Study on the Fatigue Crack Propagation Behavior of DCB Specimen with Aluminum Foam," Int. J. Precis. Eng. Manuf., Vol. 14, No. 8, pp. 1395-1399, 2013.
13. Blackman, B. R. K., Dear, J. P., Kinloch, A. J., Macgillivray, H., Wang, Y., et al., " The Failure of Fibre Composites and Adhesively-Bonded Fibre Composites under High Rates of Test Part III Mixed-mode I/II and Mode II Loadings," Journal of Materials Science, Vol. 31, No. 17, pp. 4467-4477, 1996.
14. Ohno, N., Okumura, D., and Niikawa, T., "Long-Wave Buckling of Elastic Square Honeycombs Subject to In-Plane Biaxial Compression," International Journal of Mechanical Sciences, Vol. 46, No. 11, pp. 1697-1713, 2004.
15. Sun, J. and Zhang, L., "Vehicle Actuation based Short-Term Traffic Flow Prediction Model for Signalized Intersections," Journal of Central South University, Vol. 19, No. 1, pp. 287-298, 2012.
16. Qiao, P., Wang, J., and Davalos, J. F., "Tapered Beam on Elastic Foundation Model for Compliance Rate Change of TDCB Specimen," Engineering Fracture Mechanics, Vol. 70, No. 2, pp. 339-353, 2003.
17. Michailidis, N., Stergioudi, F., Omar, H., and Tsipas, D., "An Image-based Reconstruction of the 3D Geometry of an Al Open-Cell Foam and Fem Modeling of the Material Response," Mechanics of Materials, Vol. 42, No. 2, pp. 142-147, 2010.
18. Cho, J. U., Hong, S. J., Lee, S. K., and Cho, C., "Impact Fracture Behavior at the Material of Aluminum Foam," Materials Science and Engineering: A, Vol. 539, pp. 250-258, 2012.